MIKAILALSYS
Journal of Multidisciplinary Sciences

e-ISSN : 2987-2286
p-ISSN : 2987-3924
Index: Harvard, Boston, Sydney, Copernicus, Sinta 4, Scilit, Semantic, Google, etc

https://doi.org/10.58578/mikailalsys.v4i3.12618

Mapping of Areas Affected by the Eruption of Mount Marapi in West Sumatra Using the Differential Interferometric Synthetic Aperture Radar (DInSAR) Method

Ratna Sari, Pakhrur Razi, Letmi Dwiridal, Nofi Yendri Sudiar
Universitas Negeri Padang, Indonesia
ratnasari99240@gmail.com

Submitted:	Revised:	Accepted:	Published:
Sep 28, 2026	Oct 27, 2026	Nov 7, 2026	Nov 12, 2026

Abstract

Satellite-based monitoring provides spatial information on surface changes in active volcanic regions, yet displacement patterns around Mount Marapi, West Sumatra, spanning the December 2023 eruption require further examination. This study mapped and analyzed surface displacement using differential interferometric synthetic aperture radar (DInSAR). A quantitative descriptive approach with a geospatial case study design employed two Sentinel-1A images acquired on November 28, 2023, and February 8, 2024. Processing in the Sentinel Application Platform (SNAP) included image coregistration, interferogram generation, phase filtering, phase unwrapping, and terrain correction. The results indicated spatially varying line-of-sight (LOS) displacement ranging from −0.006 to +0.460 m. Higher positive values, approximately +0.228 to +0.460 m, were concentrated around Pasie Laweh and Mount Marapi, whereas surrounding areas exhibited lower values. These estimates represent cumulative LOS changes over the acquisition interval and do not establish vertical deformation or a direct causal relationship with the eruption. The findings illustrate the potential of DInSAR to support volcanic surface monitoring and contribute spatial information for further hazard assessment. Additional satellite observations and ground-based validation are needed to strengthen displacement interpretation.

Keywords: DInSAR; Sentinel-1A; Line-of-Sight Displacement; Volcano Monitoring; Mount Marapi

Mikailalsys is licensed under a Creative Commons Attribution-NonCommercial-ShareAlike 4.0 International License

INTRODUCTION

Volcanic activity remains a persistent environmental and societal concern in regions situated along active tectonic boundaries, particularly where settlements and agricultural landscapes have developed around volcanic slopes (Ali & Jatoi, 2024; Bachri et al., 2026; Batool, 2025). Eruptions can produce ashfall, pyroclastic flows, and other volcanic materials that alter surface conditions, damage infrastructure, disrupt transportation, and threaten the livelihoods of surrounding communities. Indonesia faces considerable challenges in managing these hazards because its volcanic systems exhibit diverse geological characteristics and eruptive behaviors. Pratomo (2006) emphasized that variations in volcanic morphology and eruption history are closely associated with differences in potential hazards. Effective disaster risk reduction therefore requires reliable observations of volcanic activity alongside clear communication of hazard information to vulnerable communities (Islami et al., 2023). Advances in satellite-based monitoring have also created opportunities to observe volcanic changes across extensive and frequently inaccessible areas, contributing to a broader understanding of volcanic processes and their implications for hazard assessment (Biggs et al., 2026).

Mount Marapi, located in the Agam and Tanah Datar Regencies of West Sumatra, Indonesia, is an active volcano with an elevation of approximately 2,891 m above sea level. Its volcanic activity increased during 2023, beginning with a series of explosive eruptions between January 7 and February 20, during which eruption columns reached approximately 75–1,000 m above the summit. A more substantial explosive eruption occurred on December 3, 2023, producing an ash column approximately 3,000 m above the summit and pyroclastic flows extending roughly 3 km northward. The Geological Agency Geologi (2023) reported that this event was not preceded by a significant increase in recorded volcanic earthquakes, illustrating the challenges associated with identifying changes in volcanic conditions through individual monitoring parameters. The eruption also drew attention to atmospheric disturbances associated with volcanic ash dispersion, as investigated by Rohman et al. (2024) in the vicinity of Minangkabau Airport. These circumstances highlight the importance of examining the spatial characteristics of surface changes associated with volcanic activity, particularly in areas where communities and infrastructure may be exposed to recurring hazards.

Surface deformation represents an important physical expression of processes occurring within volcanic systems. Changes in subsurface pressure, magma migration, hydrothermal activity, and structural adjustments may produce measurable displacement at the Earth's surface, commonly expressed as uplift, subsidence, or lateral movement. Dzurisin (2007) explained that geodetic observations provide valuable evidence for interpreting volcanic behavior because deformation patterns may reflect changes within subsurface volcanic systems. Conventional monitoring instruments, including Global Navigation Satellite System (GNSS) receivers and tiltmeters, can provide precise measurements at established observation points. Their spatial coverage, however, depends on the distribution and accessibility of monitoring stations, which may be limited by steep terrain and hazardous conditions. Ebmeier et al. (2018) demonstrated that satellite observations can complement ground-based monitoring by revealing deformation patterns over extensive volcanic regions, including locations beyond the immediate summit area. More recent developments have strengthened the contribution of satellite radar observations to volcanic surveillance, although the interpretation of deformation still requires careful consideration of the geological setting and available supporting evidence (Biggs et al., 2026).

Satellite remote sensing offers a practical means of observing surface conditions across geographically extensive areas without requiring continuous physical access to the terrain. Synthetic Aperture Radar (SAR) is particularly suitable for volcanic environments because it operates as an active microwave sensing system capable of collecting observations during both daytime and nighttime and through cloud cover. According to Lillesand et al. (2015), remotely sensed observations provide spatial information that can support environmental interpretation and the identification of changes occurring across the Earth's surface. The Sentinel-1 mission, developed by the European Agency (2013), provides radar observations suitable for interferometric applications. Differential Interferometric Synthetic Aperture Radar (DInSAR) extends this capability by comparing phase information from SAR images acquired over the same geographical area at different times. After accounting for topographic and other relevant phase contributions, the resulting interferometric measurements can be used to estimate surface displacement along the radar's line-of-sight (LOS) direction. Hanssen (2001) established the theoretical basis for interpreting interferometric displacement while emphasizing the influence of measurement geometry and phase-related errors on the reliability of derived deformation estimates.

Reliable DInSAR analysis depends not only on the availability of suitable radar observations but also on appropriate image selection, processing procedures, and interpretation of interferometric quality. Sentinel-1 Single Look Complex (SLC) products retain phase information required for interferometric processing, whereas Ground Range Detected (GRD) products are primarily designed for applications involving radar backscatter characteristics. Amriyah et al. (2019) examined differences between these Sentinel-1 data products and demonstrated the relevance of selecting appropriate data types and processing software for particular analytical purposes. Interferometric processing generally involves image coregistration, interferogram generation, removal of topographic phase contributions, filtering, phase unwrapping, and geocoding. Pepe (2012) discussed the importance of phase-unwrapping techniques in resolving phase ambiguities that can influence deformation estimates. The applicability of DInSAR has also been demonstrated by (Razi et al., 2020), who used Sentinel-1A/B observations to identify spatially distributed surface deformation associated with the 2018 Lombok earthquakes. Nevertheless, atmospheric disturbances, temporal decorrelation, vegetation changes, and steep topography can introduce uncertainties that must be considered before interferometric signals are interpreted as physical ground displacement (Ebmeier et al., 2018; Hanssen, 2001).

Previous investigations of volcanic deformation in Indonesia provide empirical support for applying DInSAR to active volcanic environments. Taufik & Aprillisa (2019) examined deformation associated with Mount Bromo's eruptive activity between December 2015 and February 2016 using Sentinel-1A imagery and a two-pass DInSAR approach. Their findings indicated spatial variations in LOS displacement around the volcanic caldera, with subsidence during periods of increased activity and subsequent uplift during the observation period. A related investigation by Nugraini & Safitri (2022) analyzed surface deformation at Mount Agung, Bali, before its November 2017 eruption. The study identified uplift of approximately 4–5 cm near the summit and Budakeling area, alongside subsidence of approximately 4–5 cm around Sukadana. These investigations suggest that satellite interferometry can reveal spatially differentiated deformation patterns associated with volcanic activity. Their findings also demonstrate that deformation may extend beyond the immediate crater area, making spatial analysis relevant to understanding the geographical distribution of surface changes around active volcanoes.

Research conducted in other Indonesian geological settings has further demonstrated the usefulness of DInSAR for identifying changes in ground displacement. Azhari et al.

(2020), for example, applied DInSAR to investigate surface deformation associated with the August 2018 Lombok earthquake, illustrating its potential for documenting spatially variable ground movement. More directly related to Mount Marapi, Deshafa & Namigo (2026) analyzed volcanic deformation surrounding the December 3, 2023 eruption using Sentinel-1A observations acquired between October 23, 2023 and January 15, 2024. Their investigation identified successive deformation phases, including pre-eruption deflation, inflation, and subsequent deflation. Umniyyah et al. (2026) also investigated surface deformation at Mount Marapi using Sentinel-1 imagery covering January 2023 to March 2025. These studies provide an important basis for understanding how radar interferometry has been applied to Mount Marapi. They also establish the need to position subsequent investigations around clearly defined observation periods, specific spatial outputs, and carefully stated interpretations rather than treating the application of DInSAR to this volcano as an entirely unexplored research topic.

Existing evidence demonstrates the value of satellite interferometry for volcanic deformation studies, yet the interpretation of areas affected by an eruption requires a distinction between measurable surface displacement and the full geographical extent of disaster impacts. Interferometric displacement maps represent changes projected along the radar viewing direction and may not directly indicate damaged settlements, ashfall distribution, or the boundaries of pyroclastic deposits. Moreover, radar coherence can deteriorate where vegetation, volcanic deposits, or surface scattering properties change between acquisitions, potentially limiting the spatial completeness of the resulting deformation estimates (Hanssen, 2001; Ebmeier et al., 2018). The present investigation adopts a focused observation window extending from November 2023 to February 2024, thereby examining surface conditions before and after the December 3 eruption within a single comparative framework. Its intended contribution lies in presenting and interpreting the geographical distribution of radar-detectable surface changes during this interval, while acknowledging the temporal and measurement limitations inherent in DInSAR observations. This emphasis complements previous investigations of Mount Marapi's deformation chronology and longer-term volcanic behavior (Deshafa & Namigo, 2026; Umniyyah et al., 2026).

The present study aims to map and analyze areas surrounding Mount Marapi, West Sumatra, that exhibit detectable surface changes across the December 3, 2023 eruption period using the Differential Interferometric Synthetic Aperture Radar (DInSAR) method.

Sentinel-1A SAR imagery acquired in November 2023 and February 2024 is used to represent pre-eruption and post-eruption observation conditions, respectively. The satellite data are obtained from the Alaska Satellite Facility (ASF) and processed using the Sentinel Application Platform (SNAP) to investigate the spatial distribution and characteristics of interferometrically derived surface displacement. Particular attention is given to identifying areas showing measurable changes in LOS displacement and interpreting their spatial patterns in relation to the volcanic setting. The resulting maps are intended to provide complementary geospatial information for understanding post-eruption surface conditions and supporting volcanic hazard assessment in West Sumatra, without equating radar-detected displacement directly with independently verified physical damage.

METHODS

This study employed a quantitative descriptive approach using a geospatial case study design to examine surface deformation associated with the December 3, 2023 eruption of Mount Marapi, West Sumatra, Indonesia. The quantitative approach was selected because Differential Interferometric Synthetic Aperture Radar (DInSAR) enables the estimation and spatial representation of surface displacement from differences in radar phase measurements. The study area is located at approximately 0°22'47.72" S and 100°28'16.71" E, at an elevation of 2,891 m above sea level, covering parts of Agam and Tanah Datar Regencies. The observational coverage comprised the Mount Marapi area represented in Sentinel-1A imagery, while the satellite acquisitions were purposively selected to capture conditions before and after the eruption. Two Level-1 Single Look Complex (SLC) images acquired on November 28, 2023, and February 8, 2024, were used, representing an observation interval of 72 days. Both datasets were acquired in Interferometric Wide (IW) mode, with VV polarization and ascending orbit geometry. The images were obtained from the Alaska Satellite Facility (ASF), while Shuttle Radar Topography Mission (SRTM) Digital Elevation Model (DEM) data supported geometric processing and topographic phase correction. This design follows the principles of satellite-based deformation monitoring described by Hanssen (2001) and is consistent with previous DInSAR applications for identifying spatial variations in ground displacement (Azhari et al., 2020; Razi et al., 2020).

Satellite data were processed using the Sentinel Application Platform (SNAP) through a sequence of interferometric processing procedures. The November 2023 image

was assigned as the master image, while the February 2024 image served as the slave image. Processing began with TOPSAR Split to select the relevant subswath and bursts, followed by Apply Orbit File to improve orbital information. Image coregistration was performed through Back-Geocoding using orbital parameters and DEM data, followed by Enhanced Spectral Diversity (ESD) to improve azimuth alignment between corresponding bursts. An interferogram was subsequently generated from the coregistered complex images, together with a coherence layer representing the similarity of radar signals between acquisitions. TOPSAR Deburst was applied to combine the individual bursts into a continuous image, while topographic phase removal reduced the phase contribution associated with terrain elevation. Goldstein phase filtering and multilooking were used to suppress phase noise and improve interferogram interpretability, followed by spatial subsetting to the study area. Phase unwrapping was conducted using the Statistical-Cost Network-Flow Algorithm for Phase Unwrapping (SNAPHU), allowing the wrapped phase values to be transformed into a spatially continuous phase representation. This procedure follows the interferometric processing principles discussed by Pepe (2012), particularly regarding the importance of resolving phase ambiguity in displacement estimation.

Data analysis focused on the spatial distribution and magnitude of surface displacement derived from the processed interferometric phase. The unwrapped phase was imported into SNAP and converted into relative displacement measurements using the Phase to Displacement operator. The resulting measurements represented surface movement along the satellite's line-of-sight (LOS) direction rather than direct vertical displacement. Range-Doppler Terrain Correction was subsequently applied using DEM information to transform the radar-based displacement measurements into geographically referenced raster data. The displacement raster was classified according to its value ranges, masked using interferometric coherence, and integrated with administrative boundaries to produce a spatial map of surface changes around Mount Marapi. Interferometric coherence and the spatial continuity of phase patterns were considered when interpreting the reliability of the resulting displacement distribution, although these assessments did not constitute independent ground-based validation. The analysis emphasized the identification of areas exhibiting detectable surface displacement between the two acquisition dates, while recognizing that atmospheric disturbances, temporal decorrelation, and processing uncertainties may influence the measurements (Hanssen, 2001; Ebmeier et al., 2018). Accordingly, the resulting map was interpreted as the spatial distribution of radar-detected surface changes associated with the

eruption observation period, rather than a direct representation of all physical damage caused by the volcanic event.

RESULTS

1. Sentinel-1A Data Acquisition and Preliminary Processing

The analysis of surface deformation around Mount Marapi was conducted using two Sentinel-1A satellite images acquired before and after the December 3, 2023 eruption. The first image, recorded on November 28, 2023, represented the pre-eruption observation and was designated as the master image. The second image, acquired on February 8, 2024, represented the post-eruption observation and served as the slave image. Both datasets consisted of Level-1 Single Look Complex (SLC) products acquired in Interferometric Wide (IW) mode with VV polarization and ascending orbit geometry. The temporal separation between the acquisitions was 72 days. These acquisition characteristics provided the basis for examining changes in radar phase across the observation period. The specifications of the satellite imagery are presented in Table 1.

Table 1. Characteristics of Sentinel-1A Satellite Imagery Used in the Study

Acquisition date	Product level	Mode	Polarization	Orbit direction	Image designation
November 28, 2023	Level 1	IW	VV	Ascending	Master
February 8, 2024	Level 1	IW	VV	Ascending	Slave

Based on table 1, the initial processing involved examining the spatial coverage and baseline characteristics of the selected image pair. Baseline estimation was performed to evaluate the geometric relationship between the two acquisitions and establish their suitability for subsequent interferometric processing. The baseline estimation output for the November 28, 2023, and February 8, 2024, acquisitions is presented in Figure 1. This stage provided information on the relative acquisition geometry of the master and slave images, although the numerical baseline measurements were not reported in the available results.



Figure 1. Baseline estimation of the Sentinel-1A image pair acquired on November 28, 2023, and February 8, 2024.

Based on figure 1, the selected images were subsequently processed through TOPSAR Split and orbital correction to isolate the subswath and bursts covering the Mount Marapi study area. This procedure reduced the extent of data requiring further processing while retaining the spatial coverage relevant to the investigation. Coregistration was then carried out using the Back-Geocoding operator, supported by the Shuttle Radar Topography Mission (SRTM) Digital Elevation Model with a spatial resolution of approximately 30 m. Bicubic interpolation was applied during resampling to align the corresponding image pixels. Enhanced Spectral Diversity (ESD) was subsequently used to refine azimuth alignment between overlapping bursts. The resulting coregistered imagery, presented in Figure 2, constituted the aligned image pair used for interferogram generation.

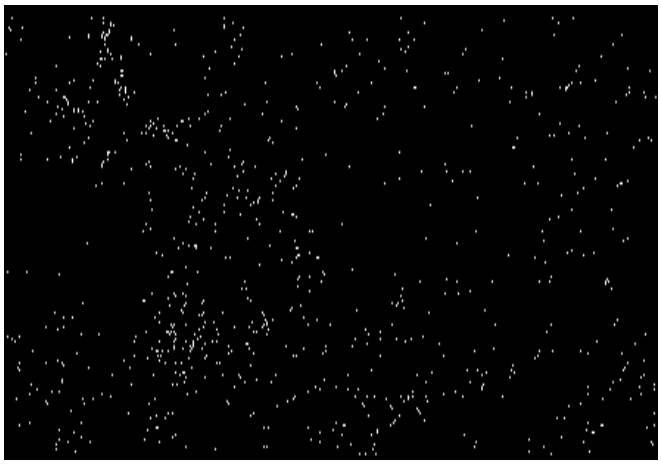


Figure 2. Coregistration results of the Sentinel-1A master and slave images covering the Mount Marapi study area.

2. Interferogram Formation, Coherence Assessment, and Phase Processing

Interferogram generation produced two principal outputs: an interferometric phase image and a coherence image. The interferometric phase represented the phase difference between the two satellite acquisitions, while the coherence image described the degree of similarity between radar signals recorded at corresponding locations.

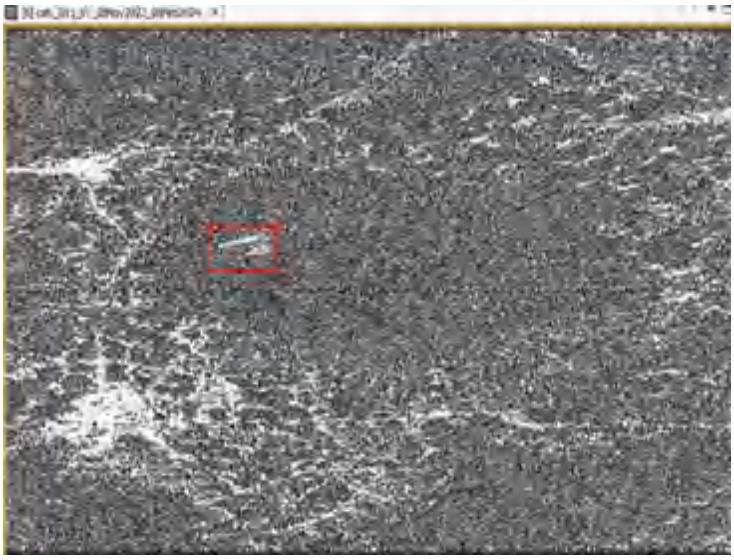


Figure 3. Interferogram and coherence images derived from the Sentinel-1A acquisitions of November 28, 2023, and February 8, 2024

Figure 3 presents the interferogram and coherence outputs obtained from the November 2023 and February 2024 image pair. These products provided the initial basis for examining the spatial continuity of radar phase information and identifying areas where the interferometric measurements could be interpreted with greater confidence. The coherence values were evaluated within a range of 0 to 1, with higher values indicating stronger similarity between the radar observations. A coherence threshold of 0.2 was adopted as the masking criterion in this study. Pixels with coherence values below 0.2 were excluded from the final displacement analysis, whereas pixels meeting or exceeding this threshold were retained. This selection reduced the inclusion of areas with particularly weak interferometric correspondence. Nevertheless, a coherence value of 0.2 or greater did not necessarily establish that the corresponding displacement measurement was free from phase noise or other sources of error. The threshold therefore functioned as a processing criterion rather than an independent measure of displacement accuracy.

The initial interferometric products contained visible boundaries between the individual TOPS bursts, appearing as horizontal discontinuities in the image display.

TOPSAR Deburst was applied to merge the bursts into a continuous raster representation. The resulting image no longer displayed the prominent burst boundaries described in the initial output. Topographic phase removal was subsequently performed using SRTM DEM information to reduce phase contributions associated with terrain elevation. The residual interferometric phase was then processed using Goldstein Phase Filtering to suppress phase noise and improve the visibility of the fringe patterns. The filtered phase output is presented in Figure 4.

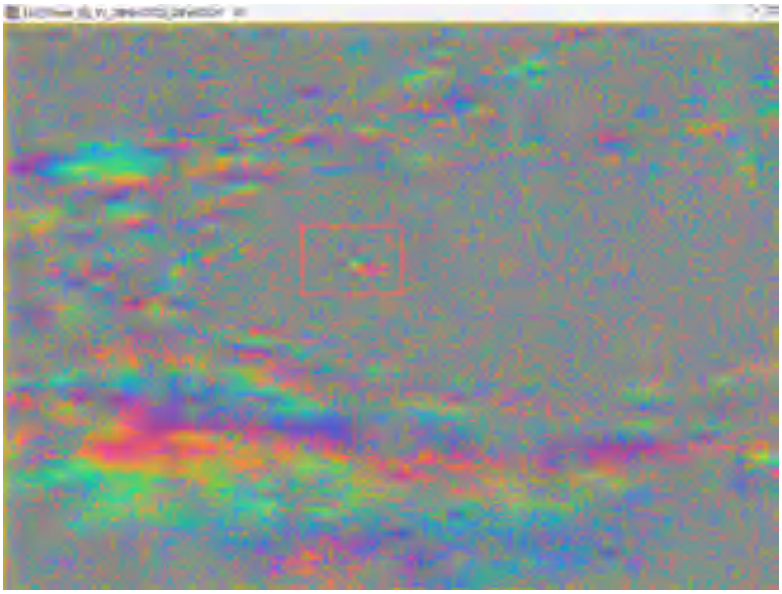


Figure 4. Interferometric phase after Goldstein phase filtering for the November 2023–February 2024 Sentinel-1A image pair

Based on figure 4, multilooking was subsequently performed to reduce speckle-related noise by combining multiple radar looks, although this process involved a reduction in spatial resolution. Spatial subsetting further restricted the interferometric products to the Mount Marapi study area. Following these procedures, phase unwrapping was undertaken to transform the phase values, initially expressed within the interval of $-\pi$ to $+\pi$ radians, into a continuous phase representation. Figure 5 presents the resulting unwrapped phase. This output provided the phase information required for calculating relative displacement, while remaining dependent on the coherence, phase continuity, and unwrapping quality of the processed interferogram.

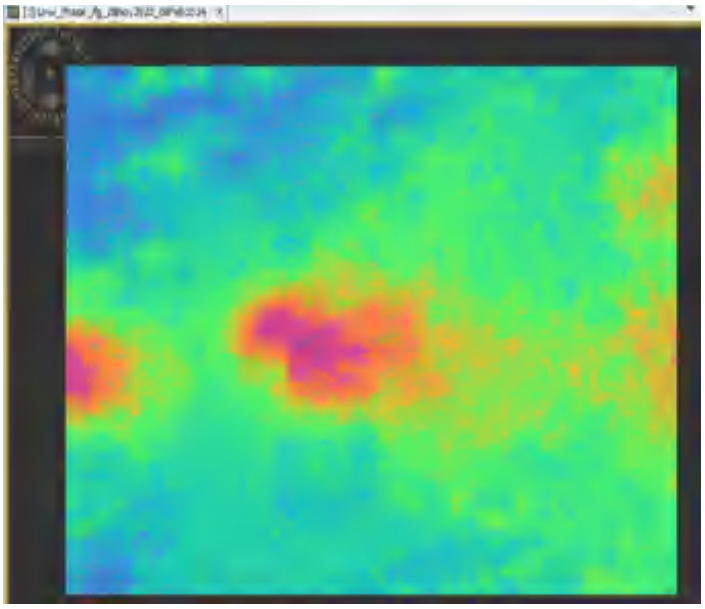


Figure 5. Unwrapped interferometric phase obtained from the Sentinel-1A image pair covering Mount Marapi

3. Line-of-Sight Surface Displacement and Geospatial Mapping

The unwrapped phase was converted into relative surface displacement using the Phase to Displacement operator in SNAP. This conversion produced a displacement raster expressed in meters along the satellite's line-of-sight (LOS) direction. The resulting values represented changes in the relative radar-to-surface distance between the two acquisition dates, rather than direct measurements of vertical ground movement. Figure 6 presents the displacement product generated from the phase conversion. This output enabled the spatial examination of displacement variations across the study area before the final geographical correction and map preparation.

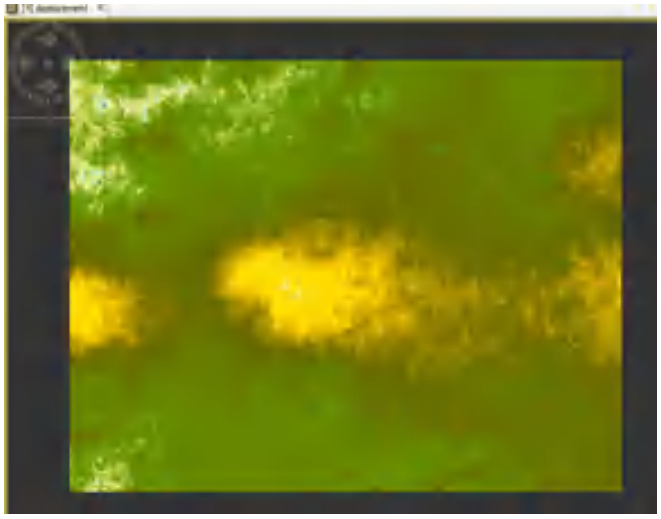


Figure 6. Line-of-sight surface displacement derived from the unwrapped interferometric phase using SNAP

Based on figure 6, Range-Doppler Terrain Correction was applied to transform the displacement raster from radar imaging geometry into geographically referenced coordinates. The correction incorporated DEM information and satellite orbital parameters to support the spatial positioning of the displacement data. Coherence masking was subsequently performed using the Band Maths function in SNAP. Pixels with coherence values below 0.2 were assigned NoData values, while those meeting the specified threshold retained their displacement measurements. The corrected and masked raster was then classified according to displacement intervals and integrated with geographic reference information. The resulting displacement layer was overlaid in Google Earth to examine its geographical coverage, before the final deformation distribution map was prepared using ArcGIS.

The final DInSAR analysis identified spatial variations in relative LOS displacement around Mount Marapi during the November 28, 2023–February 8, 2024 observation period. The reported displacement values ranged from approximately −0.006 m to +0.460 m. These measurements were grouped into five classes to illustrate the spatial variation of the results. Each class was represented by a distinct color on the deformation map, ranging from red for the lowest interval to blue for the highest interval. The classification scheme and corresponding displacement ranges are presented in Table 2.

Table 2. Classification of Line-of-Sight Surface Displacement Around Mount Marapi

Class	Color	LOS displacement range (m)	Description
1	Red	−0.006 to 0.109	Lowest displacement interval
2	Yellow	0.109 to 0.164	Lower-intermediate displacement interval
3	Green	0.164 to 0.228	Intermediate displacement interval
4	Light blue	0.228 to 0.308	Higher displacement interval
5	Blue	0.308 to 0.460	Highest displacement interval

Based on table 2, the classification indicated that displacement values were distributed unevenly across the study area. The lowest class extended from −0.006 m to 0.109 m, while the second and third classes represented values between 0.109 m and 0.228 m. The two highest classes covered displacement intervals of 0.228–0.308 m and 0.308–0.460 m, respectively. The overall range indicates considerable variation in the radar-derived displacement measurements across the mapped area. However, these values describe displacement relative to the radar observation geometry and may contain residual atmospheric, orbital, or phase-processing contributions. Their interpretation therefore requires attention to the spatial distribution and reliability of the interferometric signal.

4. Spatial Distribution of Surface Deformation Around Mount Marapi

The final deformation map, presented in Figure 7, illustrates the geographical distribution of LOS displacement around Mount Marapi across portions of Agam and Tanah Datar Regencies. The mapped displacement values formed a spatially heterogeneous pattern, with different displacement classes appearing across the western, southern, central, and eastern parts of the observation area. The distribution indicates that the measured changes in radar-to-surface distance were not uniform throughout the study region.



Figure 7. Spatial distribution of line-of-sight surface displacement around Mount Marapi, West Sumatra, derived from Sentinel-1A DInSAR analysis for November 28, 2023–February 8, 2024

Based on figure 7, the northwestern, western, and southern portions of the mapped area displayed variations predominantly within the red, yellow, and green displacement classes. These patterns were reported around Koto Tinggi, Canduang Koto Laweh, Lasi, Sariak, Bukik Batabuah, Batu Palano, Panyalaian, Paninjauan, Andaleh, and Sabu, together with parts of Talang Tangah and Gurun. The displacement intervals represented in these locations generally corresponded to the lower and intermediate classifications, extending from approximately −0.006 m to 0.228 m. The spatial variation within these settlements and surrounding landscapes indicates that the measured LOS displacement differed across locations, rather than following a single consistent pattern throughout the western and southern sectors.

The central and eastern portions of the observation area also displayed several displacement classes. Spatial variations were identified around Pasie Laweh, Tabek Patah, Tanjung Alam, Lawang Mandahiling, Salimpaung, Supayang, Rao-Rao, Padang Laweh, and Sungai Jambu. These locations formed part of the broader geographical distribution of radar-

detected surface changes surrounding Mount Marapi. The mapped variation suggests that the interferometric displacement signal was distributed across a relatively extensive area, although the available results did not establish the proportion of each administrative territory covered by individual displacement classes.

Higher LOS displacement values were particularly apparent in the central part of the study area, including the vicinity of Mount Marapi and Pasie Laweh. The light-blue class represented displacement measurements between 0.228 m and 0.308 m, whereas the blue class indicated values from 0.308 m to 0.460 m. These intervals constituted the highest displacement classes identified in the processed satellite imagery. Their concentration in parts of the central observation area distinguished these locations from sectors dominated by lower displacement values. The spatial arrangement of the higher-value classes nevertheless requires cautious interpretation because the measurements represent changes along the satellite's viewing direction and do not independently establish the physical processes responsible for those changes.

The overall findings demonstrate the capability of the applied DInSAR workflow to produce a geographically referenced representation of relative LOS displacement around Mount Marapi. The observed values ranged from −0.006 m to +0.460 m, with higher displacement classes reported predominantly in parts of the central study area and lower to intermediate classes distributed across several western, southern, and eastern locations. These results provide spatial evidence of radar-detected changes between the pre-eruption and post-eruption acquisitions. The mapped areas should therefore be understood as locations exhibiting interferometrically derived surface displacement during the observation period, rather than independently verified zones of physical damage caused by the December 3, 2023 eruption.

DISCUSSION

The DInSAR analysis identified spatial variations in surface displacement around Mount Marapi between November 28, 2023, and February 8, 2024, with values ranging from −0.006 to +0.460 m. As illustrated in Figure 7, higher displacement values (0.228–0.460 m) were concentrated in the central study area, particularly around Pasie Laweh and Mount Marapi, while surrounding locations generally exhibited lower values. This distribution indicates that surface changes were not spatially uniform throughout the observation area.

Hanssen (2001) explained that interferometric measurements represent displacement along the satellite's line-of-sight (LOS) direction rather than direct vertical movement. Therefore, the observed positive and negative values cannot independently be interpreted as volcanic inflation or deflation.

The findings are consistent with previous studies demonstrating the application of DInSAR to volcanic deformation monitoring. Taufik & Aprillisa (2019) identified spatial variations in surface deformation around Mount Bromo, while Nugraini & Safitri (2022) reported uplift and subsidence patterns around Mount Agung. Similarly, Ebmeier et al. (2018) emphasized the value of satellite radar observations for identifying volcanic deformation across extensive areas. These studies support the usefulness of DInSAR for detecting spatially distributed displacement, although differences in observation periods, satellite geometry, and processing procedures may influence the resulting measurements.

Research conducted specifically at Mount Marapi provides further context for these findings. Deshafa & Namigo (2026) identified successive deformation phases associated with the December 2023 eruption, including deflation and inflation during different observation intervals. Umniyyah et al. (2026) also examined Mount Marapi's surface deformation using a longer Sentinel-1 observation period. Unlike these investigations, the present study focused on cumulative LOS displacement between two acquisitions spanning the eruption. Consequently, the measured displacement represents changes across the entire observation period rather than deformation occurring exclusively during the December 3, 2023 event.

The spatial distribution of displacement offers useful geospatial information for volcanic monitoring and hazard assessment. Areas exhibiting higher LOS displacement may be prioritized for additional observation and comparison with geological and field-based measurements. Previous investigations by Azhari et al. (2020) and Razi et al. (2020) similarly demonstrated the applicability of DInSAR for identifying ground displacement associated with geological hazards. Nevertheless, the displacement map should not be interpreted as direct evidence of eruption-related physical damage without supporting information from independent observations.

The main limitations of this study arise from the use of a single ascending-orbit image pair separated by 72 days, the coherence threshold of 0.2, and the absence of independent ground-based validation. Atmospheric disturbances, temporal decorrelation, and phase-unwrapping errors may also affect displacement estimates (Hanssen, 2001; Pepe, 2012). The

results therefore provide an initial spatial representation of relative LOS displacement rather than definitive evidence of eruption-induced vertical deformation. Future research should incorporate additional satellite acquisitions, ascending and descending observations, and GNSS measurements to improve the reliability of deformation interpretation and strengthen its contribution to volcanic disaster risk reduction.

CONCLUSION

Based on the research findings and discussion, the application of Differential Interferometric Synthetic Aperture Radar (DInSAR) using Sentinel-1A imagery acquired on November 28, 2023, and February 8, 2024, revealed spatial variations in surface displacement around Mount Marapi, West Sumatra. The detected displacement values ranged from approximately −0.006 to +0.460 m along the satellite's line-of-sight (LOS) direction. Higher displacement values were predominantly identified in the central study area, particularly around Pasie Laweh and Mount Marapi, while several surrounding areas exhibited relatively lower values. The spatial distribution extended across locations in Agam and Tanah Datar Regencies, including Koto Tinggi, Canduang Koto Laweh, Lasi, Bukik Batabuah, Batu Palano, Tabek Patah, Tanjung Alam, Salimpaung, and Sungai Jambu. These findings indicate that surface displacement was not uniformly distributed throughout the observation area and demonstrate the potential of DInSAR for mapping spatial variations in surface conditions within volcanic environments.

The findings provide geospatial information on surface changes observed before and after the December 3, 2023 eruption of Mount Marapi. Nevertheless, the measured displacement represents relative movement along the radar's LOS direction and cannot be directly interpreted as vertical inflation or deflation. The use of a single satellite image pair also limits the ability to attribute the detected changes exclusively to the eruption. Despite these limitations, the resulting displacement map offers a useful reference for further volcanic monitoring and spatial hazard assessment. Future research should incorporate additional satellite acquisitions, both ascending and descending orbit geometries, and independent geodetic observations, such as Global Navigation Satellite System (GNSS) measurements, to improve the accuracy of displacement interpretation and better understand its relationship with volcanic activity.

REFERENCES

Ali, N., & Jatoi, S. (2024). Forces of nature: Understanding Earth's dynamic geological processes. *Asian Journal of Research in Social Sciences, 1*(2), 76–86.

Amriyah, Q., Arief, R., Dyatmika, H. S., & Maulana, R. (2019). Analysis of comparison of Level-1 data Sentinel 1A/B (SLC and GRD data) using SNAP and GAMMA software. In *Seminar Nasional Penginderaan Jauh ke-6 Tahun 2019* (pp. 533–543). https://karya.brin.go.id/id/eprint/11729/1/Prosiding_Qonita%20Amriyah_Pustekdata_2019.pdf

Azhari, M. F., Karyanto, Rasimeng, S., & Mulyanto, B. S. (2020). Analisis Deformasi Permukaan Menggunakan Metode DInSAR (Differential Interferometry Synthetic Aperture Radar) pada Studi Kasus Gempabumi Lombok Periode Agustus 2018. *JGE (Jurnal Geofisika Eksplorasi), 6*(2), 131–144. https://doi.org/10.23960/jge.v6i2.68

Bachri, S., Wibowo, S. B., Sunardi, Lavigne, F., Sumarmi, Prastiwi, M. R. H., Hakiki, A. R. R., Hidiyah, T. M., & Putri, N. R. C. (2026). Integration of topography map and land use change modeling for sustainable tourism development in Merapi Volcano, Indonesia. *Forum Geografi, 40*(2), 178–196. https://journals2.ums.ac.id/fg/article/view/12924

Badan Geologi. (2023, December 3). *Press Release Erupsi Gunung Marapi Sumatera Barat 3 Desember 2023*. https://geologi.esdm.go.id/index.php/media-center/press-release-erupsi-gunung-marapi-sumatera-barat-3-desember-2023

Batool, I. (2025). Forces of nature: Understanding Earth's dynamic geological processes. *Journal of Social Sciences, Humanities and Innovation, 1*(3), 55–63.

Biggs, J., Anantrasirichai, N., Anderson, K. R., Cayol, V., Dualeh, E. W., Dumont, Q., Ebmeier, S. K., Froger, J. L., Gaddes, M., Galetto, F., Gonzalez, P. J., Hamling, I., Hooper, A., Lazecky, M., Lizama, C. N., & Pritchard, M. E. (2026). Advances in volcano monitoring driven by the first decade of Sentinel-1 observations. *Remote Sensing of Environment, 339*, Article 115377. https://doi.org/10.1016/j.rse.2026.115377

Deshafa, A. F., & Namigo, E. L. (2026). Analisis Deformasi Vulkanik Gunung Marapi Pasca-Erupsi Desember 2023 Menggunakan Metode DInSAR Berbasis Data Sentinel-1A. *Jurnal Fisika Unand, 15*(4), 454–461. https://doi.org/10.25077/jfu.15.4.454-461.2026

Dzurisin, D. (2007). *Volcano deformation: New geodetic monitoring techniques*. Springer. https://doi.org/10.1007/978-3-540-49302-0

Ebmeier, S. K., Andrews, B. J., Araya, M. C., Arnold, D. W. D., Biggs, J., Cooper, C., Cottrell, E., Furtney, M., Hickey, J., Jay, J., Lloyd, R., Parker, A. L., Pritchard, M. E., Robertson, E., Venzke, E., & Williamson, J. L. (2018). Synthesis of global satellite observations of magmatic and volcanic deformation: Implications for volcano monitoring & the lateral extent of magmatic domains. *Journal of Applied Volcanology, 7*, Article 2. https://doi.org/10.1186/s13617-018-0071-3

European Space Agency. (2013). *Sentinel-1 user handbook*. https://filetransfer.itc.nl/pub/Dragon4_Lecturer_2018/ESA%20EEs%20and%20Sentinels%20Brochures%20pdf/Copernicus%20Sentinels%201,2,3/Sentinel-1%20User%20Handbook.pdf

Hanssen, R. F. (2001). *Radar interferometry: Data interpretation and error analysis*. Kluwer Academic Publishers. https://doi.org/10.1007/0-306-47633-9

Islami, H. S., Widana, I. D. K. K., & Subiyanto, A. (2023). Pemanfaatan Sistem Peringatan Dini Erupsi Gunung Merapi sebagai Upaya Pengurangan Risiko Bencana guna Mendukung Keamanan Nasional. *Jagratara: Journal of Disaster Research, 1*(1), 1–8. https://doi.org/10.36080/jjdr.v1i1.106

Lillesand, T. M., Kiefer, R. W., & Chipman, J. W. (2015). *Remote sensing and image interpretation* (7th ed.). John Wiley & Sons. https://www.wiley.com/en-us/remote-sensing-and-image-interpretation-7th-edition-p-9781118343289

Nugraini, L. D. A., & Safitri, D. A. (2022). Analisis Deformasi Gunung Agung Berdasarkan Data Citra SAR Sentinel-1A dan Metode D-InSAR. *Jurnal Ilmiah Geologi Pangea, 9*(1sp), 28–33. https://doi.org/10.31315/jigp.v9i1sp.9407

Pepe, A. (2012). Advanced multitemporal phase unwrapping techniques for DInSAR analyses. In I. Padrón (Ed.), *Recent interferometry applications in topography and astronomy* (pp. 57–82). IntechOpen. https://doi.org/10.5772/34224

Pratomo, I. (2006). Klasifikasi Gunung Api Aktif Indonesia, Studi Kasus dari Beberapa Letusan Gunung Api dalam Sejarah. *Indonesian Journal on Geoscience, 1*(4), 209–227. https://doi.org/10.17014/ijog.1.4.209-227

Razi, P., Sumantyo, J. T. S., Widodo, J., Izumi, Y., & Perissin, D. (2020). Land deformation monitoring using D-InSAR technique during Lombok earthquake observed by Sentinel-1A/B. *International Journal of GEOMATE, 19*(73), 257–262. https://doi.org/10.21660/2020.73.37542

Rohman, M. F., Kusmawati, A., Sena, G. Z. A., & Apriliansyah, M. S. (2024). Konseling Behavioral terhadap Remaja yang Kecanduan Alkohol akibat Broken Home. *Concept: Journal of Social Humanities and Education, 3*(1), 130–140. https://doi.org/10.55606/concept.v3i1.968

Taufik, M., & Aprillisa, I. V. (2019). Analisis Deformasi Gunung Bromo akibat Aktivitas Erupsi pada Desember 2015–Februari 2016 Menggunakan Teknologi Differential Interferometry Synthetic Aperture Radar (DInSAR). *Geoid, 14*(2), 23–27. https://iptek.its.ac.id/index.php/geoid/article/view/3866

Umniyyah, U., Arini, D., Fajrin, & Driptufany, D. M. (2026). Pemetaan Deformasi Gunung Api Menggunakan Metode Diffrential Interferometry Syntetic Aperature Radar (DInSAR): Studi Kasus Gunung Marapi, Sumatera Barat. *Jurnal Sains dan Ilmu Terapan, 9*(1), 67–76. https://doi.org/10.59061/jsit.v9i1.1362